INTERNATIONAL JOURNAL FOR NUMERICAL AND ANALYTICAL METHODS IN GEOMECHANICS, VOL. 4, 1-23 (1980)

FINITE ELEMENT ANALYSES OF ISOTROPIC AND ANISOTROPIC COHESIVE SOILS WITH A VIEW TO CORRECTLY PREDICTING IMPENDING COLLAPSE

C. T. TOH†
CSIRO, Division of Applied Geomechanics
AND
S. W. SLOAN†
Cambridge University, Cambridge, England

SUMMARY

One major problem encountered when using the finite element method to simulate the load–deformation behaviour of an elasto-plastic soil mass is that the theoretical collapse load is generally exceeded, and in some cases the numerical solution fails to exhibit a collapse load. A mixed variational principle is used as the basis for developing the governing equations of deformation and the results from this are compared with those obtained from the use of the virtual power equation. The former is found to give improved results and is generalized to include description of finite deformation. An Eulerian frame of reference is used. The method of approximating configuration changes in the numerical solution procedure is found to determine the shape of the load–deformation curve. Finally, a simple method of accounting for anisotropy of yield is presented.

1. INTRODUCTION

Although a wealth of literature exists on finite element studies of elasto-plastic continua, few have examined the ability of the method to correctly predict collapse load solutions. Comparison of numerical results with analytically obtained values has, generally speaking, been restricted to trivial cases. Commonly quoted examples include the expansion of a thick-wall cylinder and the loading of a 'V'-notched tensile block. These problems, because of the relatively simple stress-states at failure, give good correlation with analytically obtained solutions even though relatively coarse meshes are used or relatively unrefined methods of analysis are employed.

In problems concerning earthen masses, where the kinematics of deformation are much more complicated, the inaccuracy of the method in the plastic range becomes apparent. Indeed in problems of footings it is commonplace for the numerically obtained collapse load to exceed the known true collapse load by a considerable margin or, equally typically, for the numerical solution to exhibit no limit load at all.

Hence, among older publications, it is common to assume failure as having occurred whenever the iterative scheme employed fails to converge within a prescribed (maximum) number of iterations.

† Formerly Monash University, Melbourne, Australia.

0363-9061/80/0104-0001$01.00

Received 20 August 1978
Revised 12 February 1979

Attempts to improve this situation have led to the use of reduced integration schemes in conjunction with higher-order elements, e.g. Zienkiewicz, *et al.*,[1] or the use of special rupture elements which allow the violation of compatibility, e.g. Rowe and Davis,[2] or the use of mixed variational principles, e.g. Nagtegaal *et al.*[3]

This paper is concerned with correctly simulating the load–deformation characteristics of soft, elasto-plastic purely cohesive soils obeying the assumptions of infinitesimal or finite deformation. Soils exhibiting anisotropy of yield are also considered.

A general virtual power equation employing an Eulerian frame of reference is combined with the concept of instantaneous linearity to develop the governing equations. In order to examine the improvement in accuracy due to the use of penalty functions, the mixed variational principle proposed by Nagtegaal *et al.*[3] is generalized to include a description of finite deformation, and the results obtained from using the virtual power equation and the mixed variational principle are compared. Spatial integration is achieved through use of the linear isoparametric quadrilateral element.

In the case of finite deformation, it will be shown that different methods of approximating configuration changes can result in different load–deformation characteristics.

Finally, a simple method for accounting for anisotropy of yield is presented. This procedure rests on the use of the equations for an isotropic material, subject to minor stress transformations.

2. A RATE APPROACH

In plasticity theory, the entire deformation process is approximated by a series of incremental steps within which linearity is assumed. An alternative view is to consider the deformation process from time 0 to time t as a flow process, assuming instantaneous linearity. For problems where strains are no longer infinitesimal or geometry changes are no longer insignificant, three additional conditions must be satisfied:

(i) a consistent frame of reference, to which all static and kinematic variables are referred, must be employed;

(ii) all constitutive laws must relate tensors which satisfy the Principle of Material Frame Indifference (or Objectivity);

(iii) the assumption of linear decomposition of strains into elastic and plastic components is valid.

In many applications, the Lagrangian approach would be more advantageous than an Eulerian scheme since, in the former, the boundary conditions and configuration are well defined. In the latter, the geometric variables are not known *a priori*. In the field of soil mechanics, however, the loading procedure often takes the form of addition or removal of material, thus making the definition of the undeformed configuration vague.

Indeed in previous studies of the effects of accounting for finite deformation in a deforming soil mass, moving coordinate systems have been preferred, e.g. Carter *et al.*[4] and Toh[5] used an Eulerian rate approach, while Davidson and Chen[6] used a moving coordinate system which appears to be a hybrid of the Lagrangian and Eulerian schemes. The correctness of the latter method cannot be fully appreciated since no iterative scheme was used to check the degree of equilibrium satisfaction.

Most previous work employing the finite element method to solve problems involving both geometric and material non-linearity has assumed either plane stress or plane strain conditions. Notable exceptions are those by Phan *et al.*[7] and Desai and Phan[8] who employed a fully three-dimensional approach.

In an Eulerian frame of reference, the instantaneous motion of a body is described by a velocity field, $v_i(x_j, t)$, associated with the instantaneous location of each particle. The difference in velocity between adjacent points x_i and $x_i + \mathrm{d}x_i$ is given by

$$\mathrm{d}v_i = (d_{ij} + \Omega_{ij})\,\mathrm{d}x_j \tag{1}$$

where

$$d_{ij} = \frac{1}{2}\left(\frac{\partial v_i}{\partial x_j} + \frac{\partial v_j}{\partial x_i}\right) \tag{2}$$

is the rate of deformation tensor and

$$\Omega_{ij} = \frac{1}{2}\left(\frac{\partial v_i}{\partial x_j} - \frac{\partial v_j}{\partial x_i}\right) \tag{3}$$

is the spin tensor.

A small increment of displacement is obtained from

$$\mathrm{d}u_k = v_k\,\mathrm{d}t \tag{4}$$

and similarly the natural strain increment is given by

$$\mathrm{d}\varepsilon_{km} = d_{km}\,\mathrm{d}t \tag{5}$$

The total natural strain increment from time $(0)t$ to time $(n)t$ is expressed as

$$\varepsilon_{km} = \int_{(0)t}^{(n)t} d_{km}\,\mathrm{d}t = \int_{(0)t}^{(1)t} d_{km}\,\mathrm{d}t + \int_{(1)t}^{(2)t} d_{km}\,\mathrm{d}t + \cdots \int_{(n-1)t}^{(n)t} d_{km}\,\mathrm{d}t \tag{6}$$

where the integral is evaluated by following a particle through its motion and evaluating the integrand for a given particle at each time t.

Prager[9] showed that although a host of definitions of stress rates (e.g. Treusdell,[10] Cotter and Rivlin,[11] Green[12]) satisfy the Principle of Objectivity, the vanishing of the stress rates does not imply stationarity of the stress invariants. Prager[9] concluded that only the Jaumann[13] stress rate is acceptable, this being given by

$$\sigma_{ij}^{\mathrm{J}} = \dot{\sigma}_{ij} - \sigma_{ik}\Omega_{jk} - \sigma_{jk}\Omega_{ik} \tag{7}$$

where the superior dot indicates material derivative.

In the work described in this paper, the classical constitutive laws of elasticity and elasto-plasticity will be used to relate the objective stress rate tensor to the rate of deformation tensor in the following manner:

$$\sigma_{ij}^{\mathrm{J}} = C_{ijkl}d_{kl} \tag{8}$$

3. THE VIRTUAL POWER PRINCIPLE

Assuming a state of equilibrium at time $(k)t$ and applying a virtual velocity δv_i, the virtual power equation can be written as

$$\int_{(k)t_V} {}^{(k)t}F_i\delta v_i\,\mathrm{d}V + \int_{(k)t_A} {}^{(k)t}T_i\delta v_i\,\mathrm{d}A = \int_{(k)t_V} {}^{(k)t}\sigma_{ij}\delta d_{ij}\,\mathrm{d}V \tag{9}$$

where the superscripts denote the time of the event. Additionally,

$$\int_{(k)t_V} {}^{(k)t}\sigma_{ij}\delta d_{ij}\,\mathrm{d}V = \int_{(k)t_V}\left\{{}^{(k-1)t}\sigma_{ij} + \int_{(k-1)t}^{(k)t}\dot{\sigma}_{ij}\,\mathrm{d}t\right\}\delta d_{ij}\,\mathrm{d}V \tag{10}$$

and

$$\int_{(k)t_V} {}^{(k)t}F_i\delta v_i\,\mathrm{d}V = \int_{(k)t_V}\left\{{}^{(k-1)t}F_i + \int_{(k-1)t}^{(k)t}\dot{F}_i\,\mathrm{d}t\right\}\delta v_i\,\mathrm{d}V \tag{11}$$

and

$$\int_{(k)t_A} {}^{(k)t}T_i\delta v_i\,\mathrm{d}A = \int_{(k)t_A}\left\{{}^{(k-1)t}T_i + \int_{(k-1)t}^{(k)t}\dot{T}_i\,\mathrm{d}t\right\}\delta v_i\,\mathrm{d}A \tag{12}$$

Including equation (8) with equations (9) to (12), the complete equation which describes the deformation process from time $(k-1)t$ to time $(k)t$ can be written as

$$\int_{(k)t_V}\left\{{}^{(k-1)t}\sigma_{ij} + \int_{(k-1)t}^{(k)t}(C_{ijkl}d_{kl} + \sigma_{ik}\Omega_{jk} + \sigma_{jk}\Omega_{ik})\right\}\delta d_{ij}\,\mathrm{d}V$$
$$= \int_{(k)t_A}\left\{{}^{(k-1)t}T_i + \int_{(k-1)t}^{(k)t}\dot{T}_i\,\mathrm{d}t\right\}\delta v_i\,\mathrm{d}A + \int_{(k)t_V}\left\{{}^{(k-1)t}F_i + \int_{(k-1)t}^{(k)t}\dot{F}_i\,\mathrm{d}t\right\}\delta v_i\,\mathrm{d}V \tag{13}$$

4. MIXED VARIATIONAL PRINCIPLE

For a purely cohesive material, Nagtegaal *et al.*[3] showed that the demand for pointwise incompressibility (as would occur at yield) results in excessive constraints on typical two- or three-dimensional elements. This was shown to enforce unreasonable kinematic constraints on modes of deformation which the continuum should be capable of exhibiting.

To enforce the condition of pointwise incompressibility, Nagtegaal *et al.*[3] introduced a mixed variational principle where the dilatational strain rate appears as an independent variable. This is akin to firstly considering the unconstrained variational principle, equation (9), and then imposing the penalty function

$$\dot{\phi} = d_{kk} \tag{14}$$

where $\dot{\phi}$ is the independent dilatational deformation rate. The Lagrange multiplier is equal to $\kappa\dot{\phi}$, where κ is the bulk modulus. This approach is similar to that formulated by Hermann[14] for the solution of problems involving incompressible or nearly incompressible elastic materials.

A generalized form of the mixed variational principle suitable for a finite deformation description is given by

$$\int_{(k)t_V}\left\{\int_{(k-1)t}^{(k)t}(C_{ijkl}d_{kl} + \sigma_{ik}\Omega_{jk} + \sigma_{jk}\Omega_{ik})\,\mathrm{d}t\right\}\delta d_{ij}\,\mathrm{d}V + \int_{(k)t_V}\left\{\int_{(k-1)t}^{(k)t}\kappa(d_{kk} - \dot{\phi})\,\mathrm{d}t\right\}\delta\dot{\phi}\,\mathrm{d}V$$
$$= \int_{(k)t_A}\left(\int_{(k-1)t}^{(k)t}\dot{T}_i\,\mathrm{d}t\right)\delta v_i\,\mathrm{d}A + \int_{(k)t_V}\left(\int_{(k-1)t}^{(k)t}\dot{F}_i\,\mathrm{d}t\right)\delta v_i\,\mathrm{d}V \tag{15}$$

For the sake of convergence and, in order to overcome the excessive constraints enforced on each element due to the demand for incompressibility, it is necessary (see Negtegaal *et al.*[3]) to specify that the independent dilatational deformation rate be constant throughout each ele-

ment. This gives rise to

$$\phi_\alpha = \int_{V_\alpha} \frac{d_{kk}\,\mathrm{d}V}{V_\alpha} \tag{16}$$

where α refers to a particular element.

By redefining the rate of deformation tensor as

$$\bar{d}_{ij} = \frac{1}{2}\left(\frac{\partial v_i}{\partial x_j} + \frac{\partial v_j}{\partial x_i}\right) + \frac{1}{3}\,\delta_{ij}\left(V_\alpha^{-1}\int_{V_\alpha} d_{kk}\,\mathrm{d}V - d_{kk}\right) \tag{17}$$

the spin tensor is thus redefined as

$$\bar{\Omega}_{ij} = \frac{1}{2}\left(\frac{\partial v_i}{\partial x_j} - \frac{\partial v_j}{\partial x_i}\right) + \frac{1}{3}\,\delta_{ij}\left(V_\alpha^{-1}\int_{V_\alpha} d_{kk}\,\mathrm{d}V - d_{kk}\right) \tag{18}$$

and equation (15) can be simplified to

$$\int_{(k)t_V}\left\{\int_{(k-1)t}^{(k)t}(C_{ijkl}\bar{d}_{kl} + \sigma_{ik}\bar{\Omega}_{jk} + \sigma_{jk}\bar{\Omega}_{ik})\,\mathrm{d}t\right\}\delta d_{ij}\,\mathrm{d}V$$
$$= \int_{(k)t_A}\left(\int_{(k-1)t}^{(k)t}\dot{T}_i\,\mathrm{d}t\right)\delta v_i\,\mathrm{d}A + \int_{(k)t_V}\left(\int_{(k-1)t}^{(k)t}\dot{F}_i\,\mathrm{d}t\right)\delta v_i\,\mathrm{d}V \tag{19}$$

where

$$\sigma_{ij}^{\mathrm{J}} = C_{ijkl}\bar{d}_{kl}. \tag{20}$$

Thus the only difference between equation (19) and the incremental form of equation (13) is in the redefinition of the rate of deformation and spin tensors.

5. NUMERICAL SOLUTION PROCEDURE

5.1. Time integration

The solution of equations (13) and (19) requires that integration be performed over both space and time. While spatial integration is achieved *via* the ubiquitous finite element method, time integration can best be accomplished by approximating the continuous process as a series of small but finite time steps. This is equivalent to expanding the time dependent variables about $(k-1)t$ by a Taylor series expansion and neglecting higher-order terms; i.e.

(i) *Configuration variable*

$${}^{(k)t}x_i = {}^{(k-1)t}x_i + \{{}^{(k-1)t}\dot{x}_i\delta t + \cdots\} = {}^{(k-1)t}x_i + {}^{(k-1)t}\mathrm{d}x_i \tag{20a}$$

(ii) *Stress field*

$${}^{(k)t}\sigma_{ij} = {}^{(k-1)t}\sigma_{ij} + \{{}^{(k-1)t}\dot{\sigma}_{ij}\delta t + \cdots\} = {}^{(k-1)t}\sigma_{ij} + {}^{(k-1)t}\mathrm{d}\sigma_{ij} \tag{20b}$$

5.2. Numerical solution of the governing equations

Performing the time integration over equation (13) in the manner shown above, we obtain, in matrix form

$$\int_{(k)t_V}\delta\{d\}^{\mathrm{T}}\{\{{}^{(k-1)t}\sigma\} + [C({}^{(k)t}\sigma)]\{\Delta\varepsilon\} + [T_{\mathrm{w}}]\{{}^{(k)t}\sigma\}\} = \int_{(k)t_V}\delta\{v\}^{\mathrm{T}}\{F\}\,\mathrm{d}V + \int_{(k)t_A}\delta\{v\}^{\mathrm{T}}\{T\}\,\mathrm{d}A \tag{21}$$

In finite element terminology, equation (21) can be expressed as

$$\sum \int_{(k)tV_\alpha} ([B]^T\{^{(k-1)t}\sigma\} + [B]^T[C(^{(k)t}\sigma)][B]\{\Delta q\} + [T_w]\{^{(k)t}\sigma\})\, dV = \{R\} \tag{22}$$

where

$$\{R\} = \sum \int_{(k)tV_\alpha} [N]^T\{F_N\}\, dV + \int_{(k)tA_\alpha} [N]^T\{T_N\}\, dA \tag{23}$$

and where the summation is taken over all elements in the continuum.

In the case of equation (19), the final finite element form of the equation is similar to equation (22) except that $[B]$ and $[T_w]$ are replaced by $[\bar{B}]$ and $[\bar{T}_w]$ respectively, the explicit forms of which are given in the Appendix.

The two most common iterative schemes employed to solve the governing equations are the constant stiffness (initial stress) and the mixed (variable stiffness together with a modified Newton–Raphson procedure) methods. The principal advantage of the former is that the overall stiffness is assembled and inverted only once during the entire analysis. Further, the formulation is particularly convenient for elasto-plastic problems because unloading, work-softening and non-associated flow rules are easily catered for. Recently, however, it has been noted that convergence may be very slow once the plastic strains become large and, thus, although the constant stiffness technique may be satisfactory for situations where only moderate plastic deformation occurs, it is unsuitable if a complete load–deformation response is required. For this reason, a mixed algorithm is utilized in the present work—the stiffness is updated at the beginning of each time step and a modified Newton–Raphson procedure is used within each time step to attain an acceptable level of equilibrium.

On the Burroughs 6700 computer installation at Monash University, this procedure was found to be about 50 per cent more economical than the constant stiffness method for a typical geomechanics problem in which the entire deformation response is simulated.

To ensure economic computer storage and to indicate the stress field involved when forming the stiffness matrix at the beginning of each time step, equation (22), or the mixed variational principle, can best be expressed as

$$\begin{aligned}\sum \int_{(k)tV_\alpha} [B]^T[C(^{(k-1)t}\sigma)][B]\, dV\, \{\Delta g\} \\ = \{R\} - \sum \int_{(k)tV_\alpha} [B]^T\{^{(k-1)t}\sigma\}\, dV + \sum \int_{(k)tV_\alpha} [B]^T\{\Delta\sigma_{o/b}\}\, dV \\ - \sum \int_{(k)tV_\alpha} [B]^T[T_w]\{^{(k)t}\sigma\}\, dV\end{aligned} \tag{24}$$

where

$$\{\Delta\sigma_{o/b}\} = [C(^{(k-1)t}\sigma)] - [C(^{(k)t}\sigma)]\{\Delta\varepsilon\} \tag{25}$$

5.3. Approximations to configuration changes

Owing to the use of an Eulerian frame of reference, the configuration over which spatial integration is to be conducted is not known *a priori* and an approximation to the configuration at time $(k)t$ has to be made. Three different ways of approximating the configuration are:

(i) the geometry is updated prior to each time step and maintained constant for that time step while the iterative procedure to equilibrate the system takes place. Thus each time step begins with a new 'initial' geometry;
(ii) the geometry is continually updated throughout the iterative process, i.e. material and geometric non-linearity are considered simultaneously;
(iii) material and geometric non-linearity are considered sequentially within each time step. The geometry is updated prior to and maintained constant during the iterative procedure. Once convergence is attained, the geometry is updated and the iterative procedure repeated for a new configuration within the same time step. Usually no more than one change in geometry is required.

Depending on which of the above three procedures is used, the time superscripts in equation (24) will have to be adjusted accordingly. In the cases of sequential consideration of material and geometric non-linearity, equation (24) is approximated to

$$\sum \int_{(k-1)t_{V_\alpha}} [B]^{\mathrm{T}}[C(^{(k-1)t}\sigma)][B]\,\mathrm{d}V\,\{\Delta q\} = \{R\} - \sum \int_{(k-1)t_{V_\alpha}} [B]^{\mathrm{T}}\{^{(k-1)t}\sigma\}\,\mathrm{d}V + \sum \int_{(k-1)t_{V_\alpha}} [B]^{\mathrm{T}}\{\Delta\sigma_{\mathrm{o/b}}\}\,\mathrm{d}V - \sum \int_{(k-1)t_{V_\alpha}} [B]^{\mathrm{T}}[T_{\mathrm{w}}]\{^{(k)t}\sigma\}\,\mathrm{d}V \tag{26}$$

When geometric and material non-linearity is regarded simultaneously then equation (24) is approximated to

$$\sum \int_{(k-1)t_{V_\alpha}} [B]^{\mathrm{T}}[C(^{(k-1)t}\sigma)][B]\,\mathrm{d}V\,\{\Delta q\} = \{R\} - \sum \int_{(k)t_{V_\alpha}} [B]^{\mathrm{T}}\{^{(k-1)t}\sigma\}\,\mathrm{d}V + \sum \int_{(k)t_{V_\alpha}} [B]^{\mathrm{T}}\{\Delta\sigma_{\mathrm{o/b}}\}\,\mathrm{d}V - \sum \int_{(k)t_{V_\alpha}} [B][T_{\mathrm{w}}]\{^{(k)t}\sigma\}\,\mathrm{d}V \tag{27}$$

5.4. Other necessary refinements for accurate elasto-plastic analyses

In the analyses reported herein, the two different yield criteria used to describe cohesive behaviour are the Tresca and the von Mises yield criteria. In general the operations described below are necessary for accurate computations in the highly non-linear range.

(i) Departure of stresses from the yield surface usually occurs owing to the approximations inherent in the analysis procedure and the errors are cumulative. As it is at least desirable to preserve the yield condition, it is necessary to ensure that, at each stage, the stresses are restored to the yield surface.
(ii) The approximation to the rate constitutive law is given by

$$\{\Delta\sigma^{\mathrm{J}}\} = [C(^{(k)t}\sigma)]\{\Delta\varepsilon\}$$

An improved estimate of the stress field is obtained if the time step δt is subdivided into m time sub-steps. Thus within each iteration (where the stiffness matrix is unchanged), $\{\Delta\varepsilon\}$ is divided into m sub-intervals and thus $[C(^{(k)t}\sigma)]$ is reformed m times. Additionally, the correction for departure from the yield surface is made the same number of times. For footing problems five time sub-steps are usually adequate.

(iii) Proper estimation of the plastic strain increment at first yield.

Various methods of performing (i), (ii) and (iii) have been suggested in the literature. The algorithms adopted in the present work are similar to those proposed by Nayak and Zienkiewicz.[15]

6. ANISOTROPY OF YIELD

In a series of undrained true triaxial tests on 'undisturbed' soft sensitive Launceston clay (using abrupt changes in pore-pressure as a criterion for defining yield), Toh[5] established that the yield locus took the form of a von Mises yield criterion but with the centre shifted away from the hydrostatic axis (Figure 1).

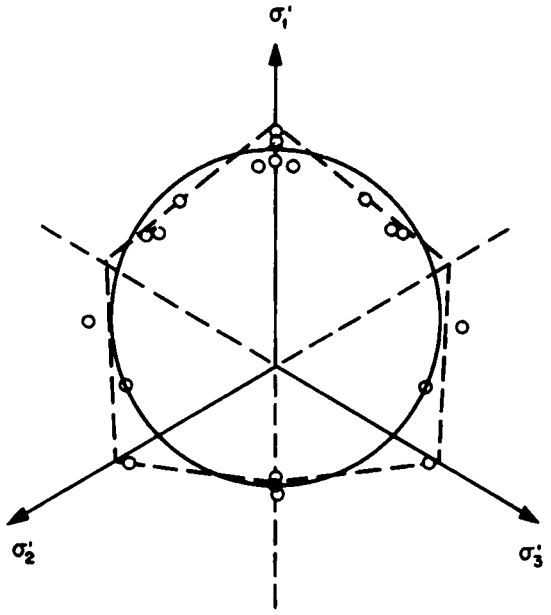

Figure 1. Possible yield surfaces (Toh[5])

The task of developing general three-dimensional elasto-plastic equations for an anisotropic material is mathematically cumbersome. Since the experimentally obtained yield locus is identical in shape to the von Mises yield criterion, the equations developed for the latter could be used to describe the former provided relevant stress transformations are invoked.

The mathematical device adopted here will rest on the assumption that the yield surface rotates along with the principal stresses for want of experimental results concerning stress rotation.

As shown in Figure 2, the yield surface, while being anisotropic in the 'real' stress space, is itself 'isotropic' in an 'artificial' stress space.

The relationships between real and artificial principal stresses are

$$\sigma_1^{\mathrm{A}} = \sigma_1^{\mathrm{R}} - (\sqrt{6}k/3) \tag{28a}$$

$$\sigma_2^{\mathrm{A}} = \sigma_2^{\mathrm{R}} + (\sqrt{6}k/6) \tag{28b}$$

$$\sigma_3^{\mathrm{A}} = \sigma_3^{\mathrm{R}} + (\sqrt{6}k/6) \tag{28c}$$

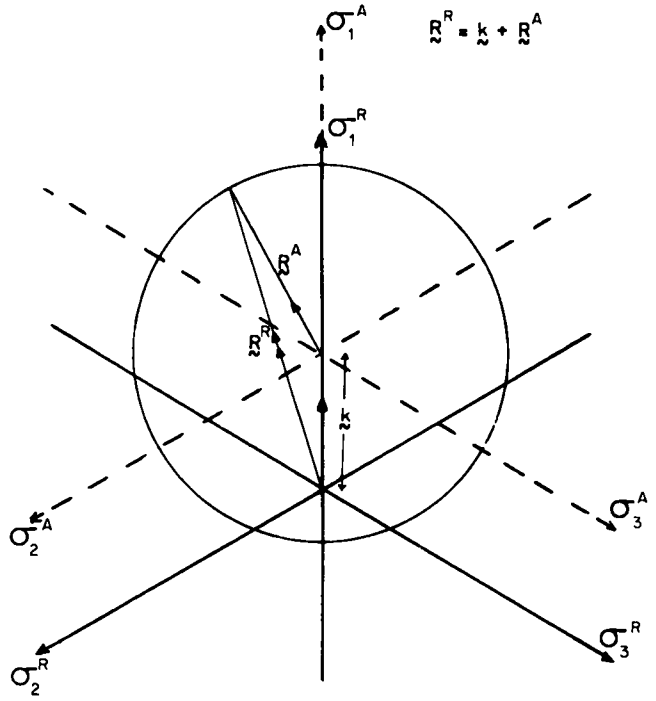

Figure 2. Relation between 'real' and 'artificial' stress space

where the superscripts A and R refer to artificial and real respectively, and k is the distance from the circle centre (hydrostatic stress axis of the artificial stress space) to the hydrostatic axis of the real stress space. Note that the subscript 1 corresponds to the vertical direction and the subscripts 2 and 3 correspond to the horizontal directions.

The use of an artificial stress space provides a convenient and compact means of defining the yield surface and the elasto-plastic constitutive law which, in its final form, is identical in both stress spaces.

The only extra steps needed to account for this type of anisotropy are simply:

(i) compute the elasto-plastic law based on the artificial stresses;
(ii) transform the real principal stresses into the artificial frame, noting that the vertical stress, σ_2, need not correspond to the major principal stress;
(iii) perform all necessary numerical procedures discussed in Section 5.4 within the artificial frame;
(iv) at the end of each iteration, transform all stresses back to the real stress space.

The introduction of this type of perfectly plastic anisotropic behaviour can result in the possibility of 'hardening' or 'softening' behaviour, depending on the post-yield direction of the stress-path, since hardening or softening is associated with an increase or decrease in the octahedral shearing stress, $\bar{\sigma}$, or the length of the vector emanating from the hydrostatic stress axes, R (radius of the isotropic von Mises circle).

This is illustrated in Figure 3 where stress-path **a** traverses so as to increase $\bar{\sigma}$ (hardening) whereas path **b** traverses in such a manner as to decrease $\bar{\sigma}$ (softening).

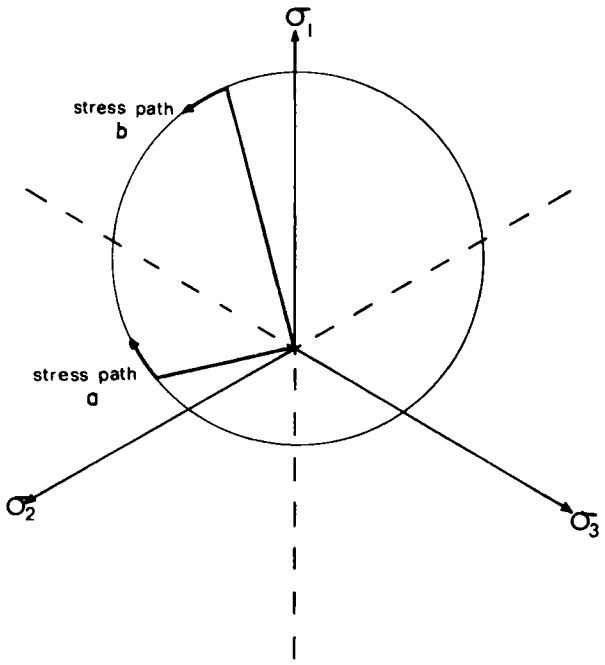

Figure 3. 'Hardening' or 'softening' behaviour associated with anisotropy

7. ALGORITHM VERIFICATION

To assess the correctness of the procedures suggested, some trivial cases of simple geometry subjected to homogeneous deformations were considered. These were:

(i) homogeneous compression of a plane-strain block for which the analytical solution was derived by Fernandez and Christian[16] (Figure 4(a) and 4(b));

(ii) expansion of an elastic cylinder (Figure 5(a) and 5(b));

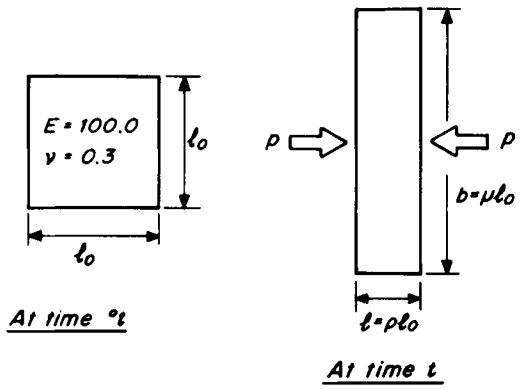

Figure 4(a). Plane strain compression of square block

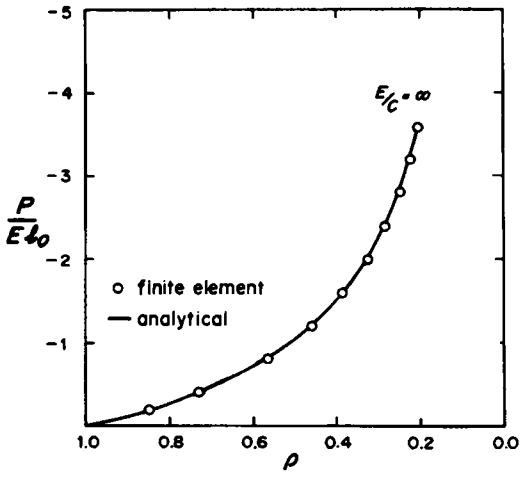

Figure 4(b). Plot of normalized force versus ratio of compressed length to original length

(iii) expansion of an elasto-plastic cylinder (Figure 6).

For such simple problems, numerical results correlate excellently with analytical solutions. In case (iii), both variational principles were used but the difference in results proved to be insignificant.

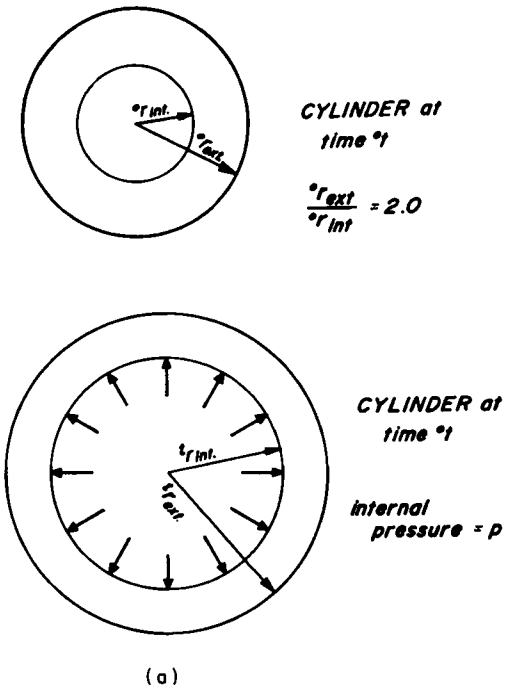

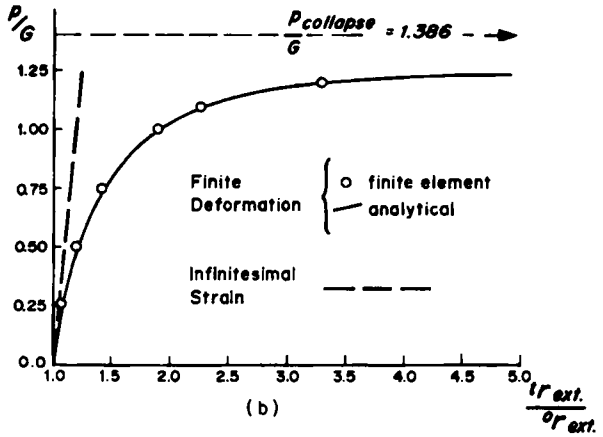

Figure 5. Elastic expansion of thick infinite cylinder subjected to internal pressure p

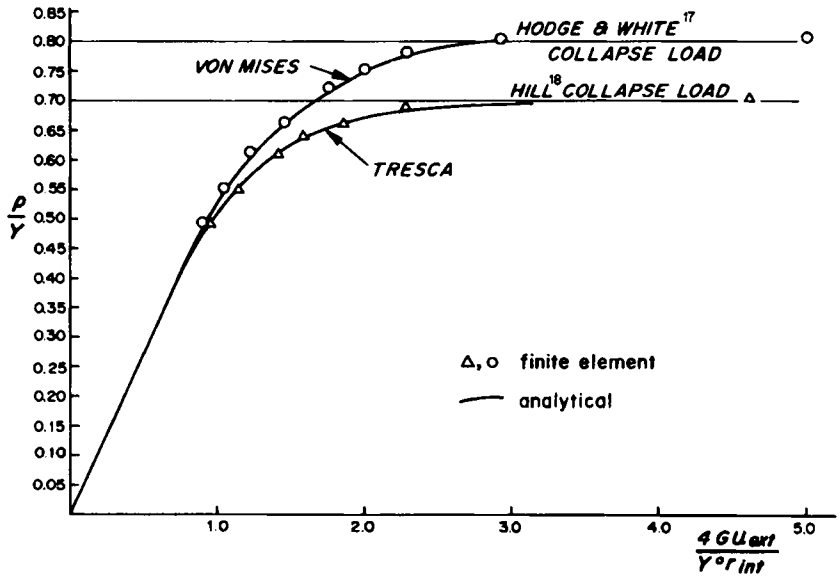

Figure 6. Pressure–deformation plot

8. GEOTECHNICAL PROBLEMS

8.1. Infinitesimal strain conditions—comparison of two variational principles

The problem of over-predicting theoretically obtained collapse loads has been recognised by a number of workers, e.g. Chen[19] and Rowe and Davis.[2]

The use of low E/c ratios ($\simeq 130$) in these calculations is deliberate. For a high E/c ratio the large difference between the elastic and the elasto-plastic slopes of the load–displacement curve tends to create an illusion of impending collapse. Nonetheless a close scrutiny of such cases would almost invariably reveal that the load–deformation curve would continue to rise beyond the limit load at virtually constant gradient.

To illustrate the difference in the use of the two variational principles, two problems involving flexible strip footings were analysed. The first concerned a thin layer of soft clay underlain by a solid rock stratum, while the second problem involved an approximation to an infinite layer of soft clay.

The results are shown in Figures 7 and 8. When the virtual power equation was utilized, no limit load is attained and the load–displacement curve continues to rise at almost a constant gradient. However, the use of the mixed variational principle produces an entirely different load–displacement curve, one that tends towards a collapse solution some 8 per cent above the theoretical collapse load. The difference between the two curves becomes apparent almost immediately after first yield.

Figure 9 illustrates that the use of time sub-steps (Section 5.4 (ii)) increases the accuracy of the analyses to the extent that only marginal improvement is obtained by increasing the number of time steps.

Owing to the vastly improved results from use of the mixed variational principle, it will be adopted for the rest of the paper.

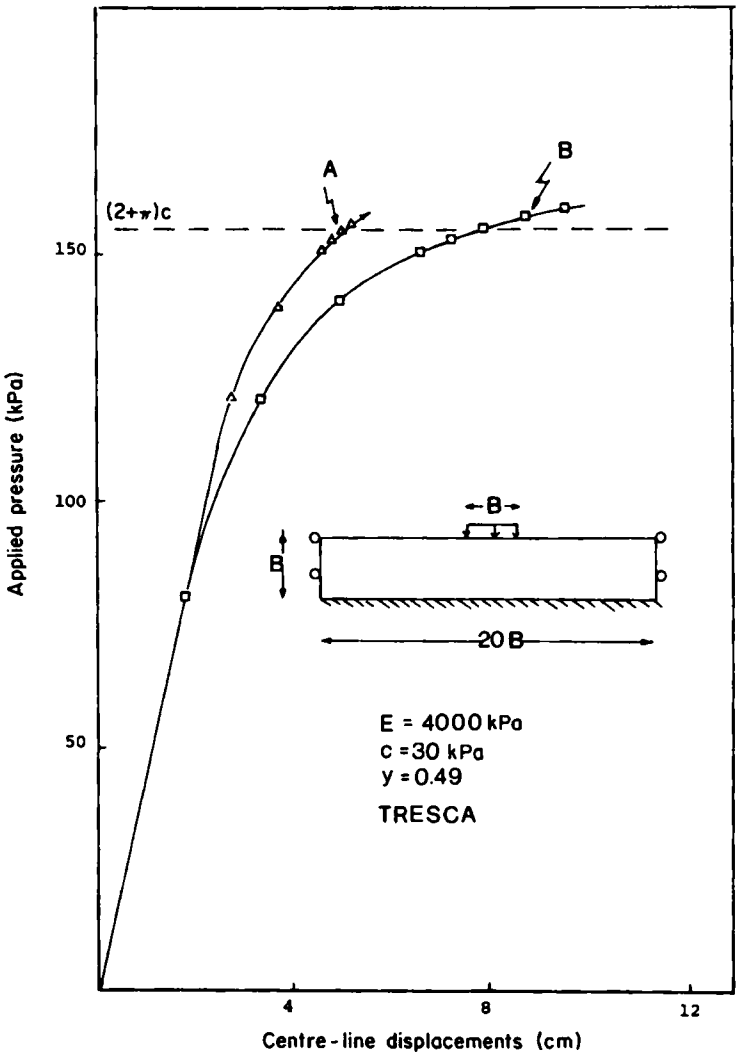

Figure 7. Load–deformation responses (infinitesimal deformation). Curve A—Load-displacement curve obtained from the virtual power equation. Curve B—Load-displacement curve obtained from the mixed variational principle

8.2. Finite deformation analysis—effects of different methods of approximating configuration changes

The effects of approximating configuration changes by the different methods proposed in Section 5.3 are illustrated in Figures 10 and 11. For comparison purposes, the corresponding results for infinitesimal strain analyses are also inserted.

Method 5.3(ii), where material and geometric non-linearity are simultaneously considered, is found to be unstable near the theoretical infinitesimal strain collapse load. The iterative procedure begins first to oscillate and then to diverge once the theoretical collapse load (infinitesimal strain) is approached. In the vicinity of unlimited settlement, no stable configuration exists for which a stress state could remain in equilibrium.

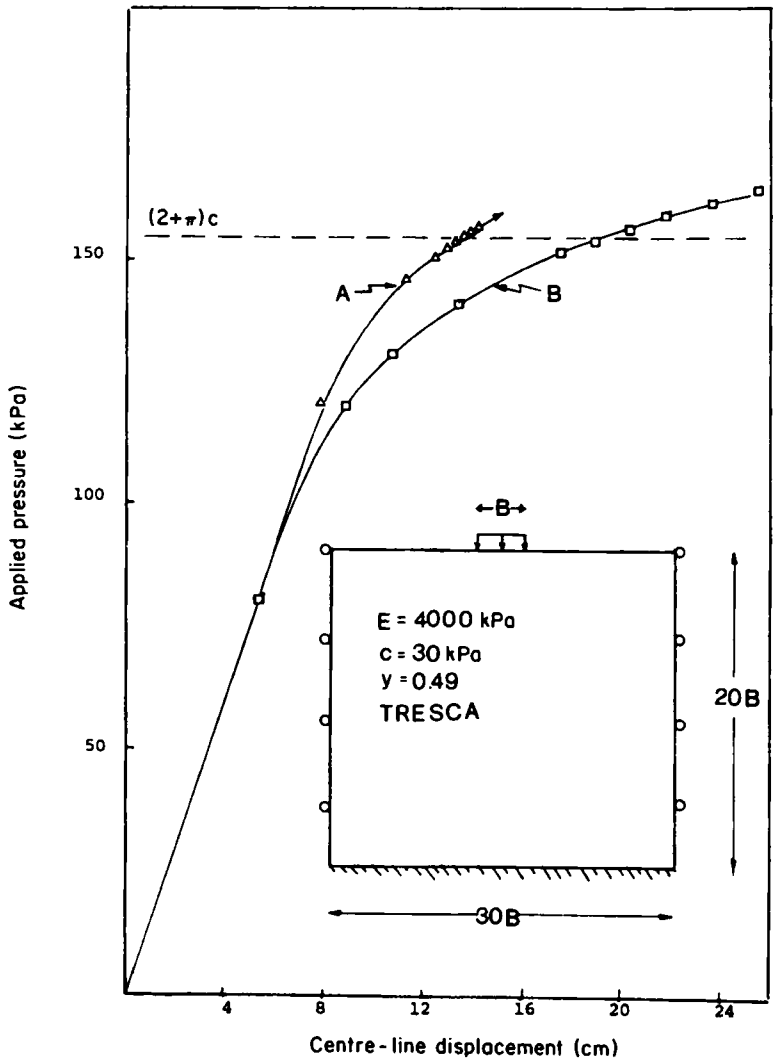

Figure 8. Load–deformation responses (infinitesimal deformation). Curve A—Load–displacement curve obtained from the virtual power equation. Curve B—Load-displacement curve obtained from the mixed variational principle

Methods 5.3(i) and 5.3(iii), where material and geometric non-linearity are sequentially considered, prove to be more numerically stable. Immediately past the theoretical infinitesimal strain collapse load, a gradual increase in the rate of hardening (slope of the load–displacement curve) is observed. In the case of the footing on a thin layer of soft clay over a rough rigid base, this phenomenon is more pronounced and thus reflects the proximity of the rigid base.

It is uncertain as to which of the three methods is the correct procedure to use. Clearly from a purely theoretical viewpoint, method 5.3(ii) provides a better approximation to the governing equations. The use of this method implies that for a cohesive soft material, the collapse load

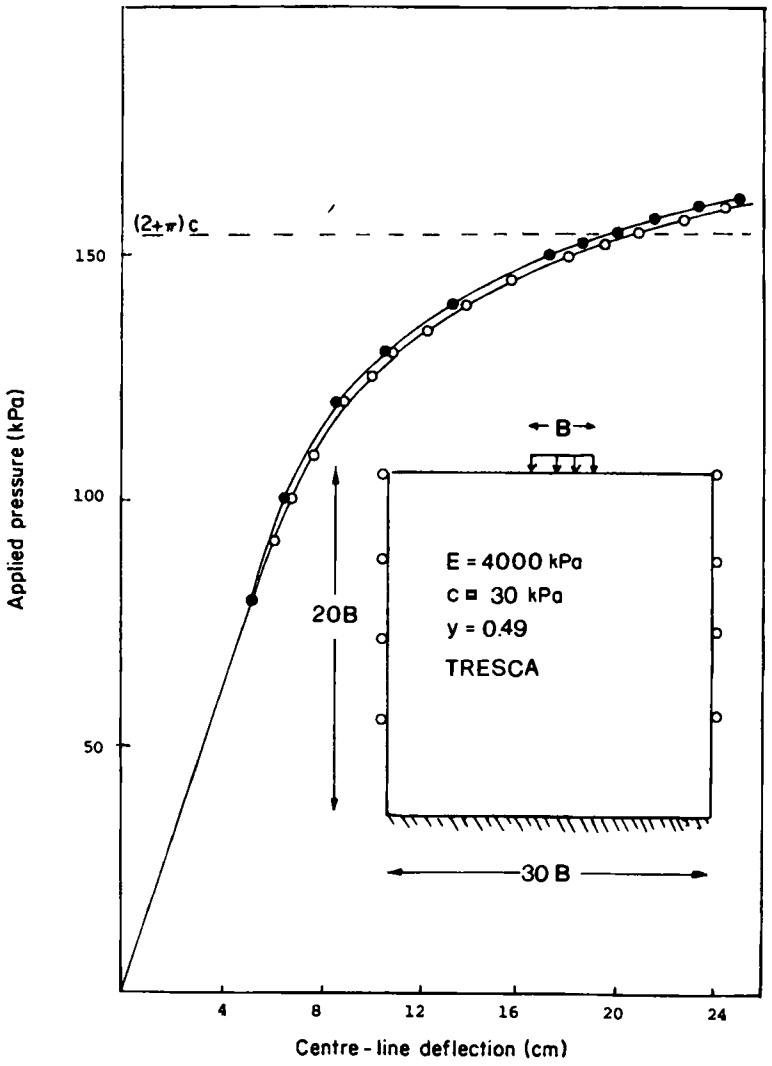

Figure 9. Load–deformation responses (infinitesimal deformation)

value for an infinitesimal strain assumption is identical to that for finite deformation, given that the finite element model is sufficiently accurate.

Another feature is that immediately past first yield, the finite deformation load–displacement curve records a softer response than the equivalent infinitesimal strain case. This is different from the results of Carter *et al.*[4] and Davidson and Chen[6] where, for this range of material properties, no difference in results between the two analyses were observed until past the theoretical collapse load where the large deformation case recorded a stiffer response. Both authors used the virtual work expression.

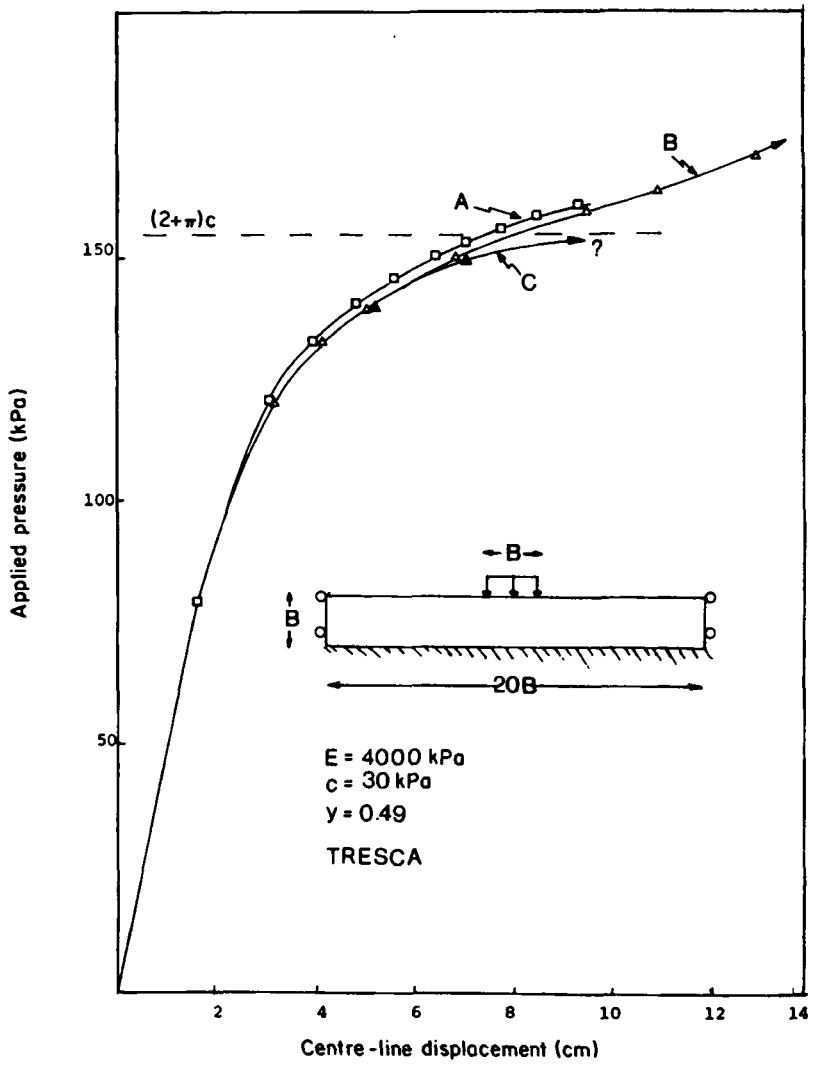

Figure 10. Load–deformation responses (infinitesimal and finite deformation). Curve A—Infinitesimal deformation analysis. Curve B—Finite deformation analysis with sequential consideration of material and geometric non-linearity. Curve C—Finite deformation analysis with simultaneous consideration of material and geometric non-linearity. Numerical scheme becomes unstable near collapse load

8.3. Materials exhibiting anisotropy of yield

To compare the differences in the deformation characteristics between an isotropic and an anisotropic material under a strip-footing, three different infinitesimal strain analyses were performed using:

(i) the anisotropic yield surface as determined by Toh[5] (see Figure 1);

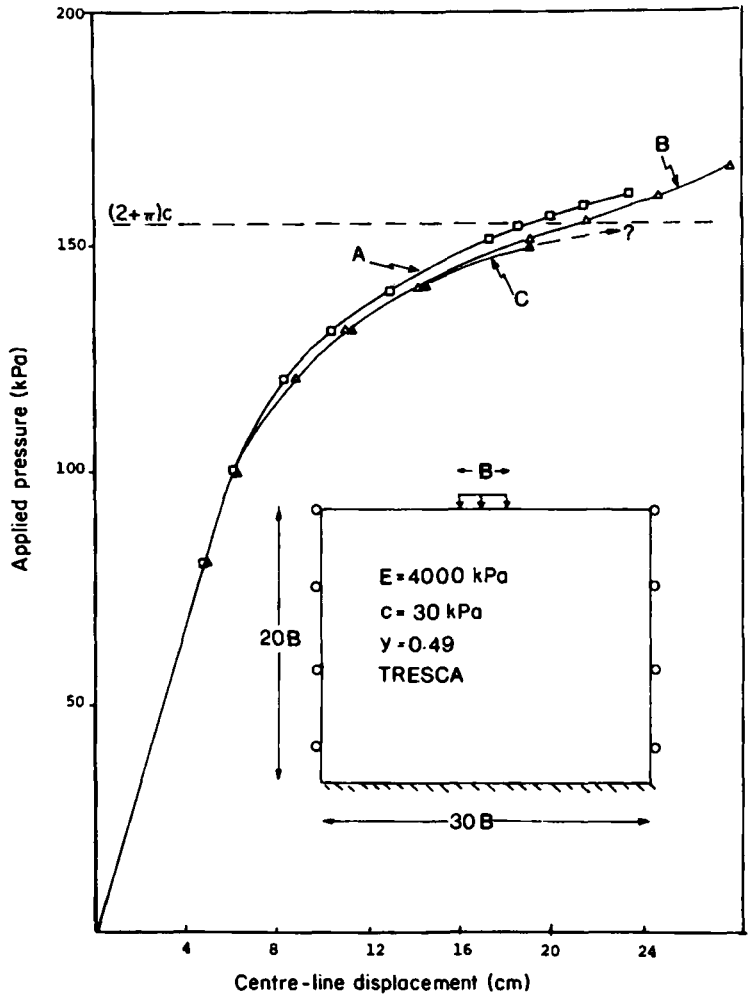

Figure 11. Load–deformation responses (infinitesimal and finite deformation). Curve A—Infinitesimal deformation analysis. Curve B—Finite deformation analysis with sequential consideration of material and geometric non-linearity. Curve C—Finite deformation analysis with sequential consideration of material and geometric non-linearity. Numerical scheme becomes unstable near collapse load

(ii) an isotropic von Mises yield surface with the cohesion equal to that at yield as determined from triaxial compression tests, $c = c_{comp}$;

(iii) an isotropic von Mises yield surface with the value of cohesion equal to the average of the yield values obtained in triaxial compression and extension tests, i.e.

$$c = \frac{c_{comp} + c_{ext}}{2}$$

The yield surface for Launceston clay, together with the equivalent one-dimensional representation, are shown in Figure 12.

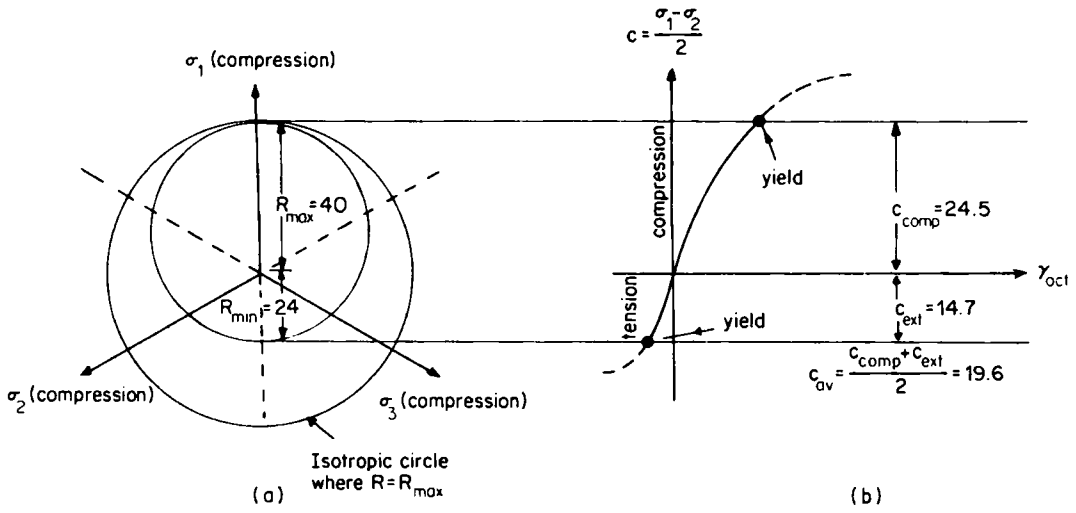

Figure 12. (a) Yield surface for Launceston clay in 3-D stress space (depth 7·5 m) (Toh[5]). (b) Equivalent one-dimensional stress–strain representation

The resulting load–displacement curves, shown in Figure 13, illustrate several notable features:

(i) the anisotropic model gave a collapse load 8 per cent lower than the theoretical collapse load for an isotropic material with $c = c_{comp}$;

(ii) the collapse load for the anisotropic model was 14 per cent higher than the theoretical value for an isotropic material with $c = (c_{comp} + c_{ext})/2$;

(iii) a comparison of the load–displacement curves for the anisotropic and the isotropic ($c = c_{comp}$) material indicates that initially the elements yield under plane strain compressive stresses, resulting in very little difference between the two models. The large difference in collapse load arises from the large difference in intermediate principal stresses.

Since the Launceston clay model was obtained from tests on samples which were anisotropically re-consolidated to field stresses, it would be consistent to apply a set of initial stresses prior to the application of surface tractions. The result (Figure 14) is a softer response with a lower collapse load.

9. CONCLUSION

One of the major conclusions that can be drawn from the work presented herein is that the method proposed by Nagtegaal *et al.*[3] can be successfully employed to predict impending collapse and is a viable alternative to traditional analyses which often require large numbers of elements.

Generally speaking there is very little difference between finite and infinitesimal strain responses for typical footing problems. Detailed comparisons are difficult owing to the fact that

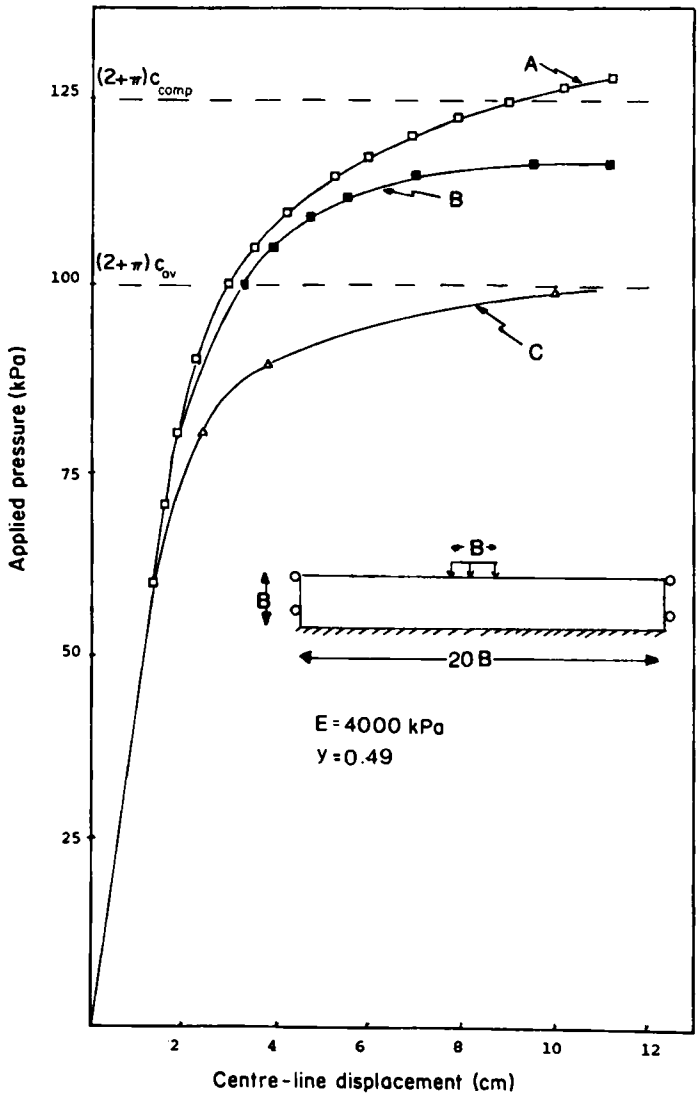

Figure 13. Load–deformation responses (infinitesimal deformation). Curve A—Load–deformation response for a perfectly plastic isotropic von Mises material with cohesion equal to that obtained in triaxial compression, i.e. $C = 24{\cdot}5$ kPa. Curve B—Load–deformation response obtained using the perfectly plastic, anisotropic Launceston clay model. Curve C—Load–deformation response for a perfectly plastic von Mises material with cohesion equal to the average obtained from triaxial compression and extension tests, i.e. $c = (c_{comp} + c_{ext})/2 = 14{\cdot}7$ kPa

the different methods of accounting for geometric non-linearity result in different predicted load responses.

The method for accounting for anisotropy of yield can be incorporated into existing finite element programmes with minimal programming modifications. The use of the anisotropic model results in a load–displacement curve which more clearly defines a collapse load than an isotropic yield surface.

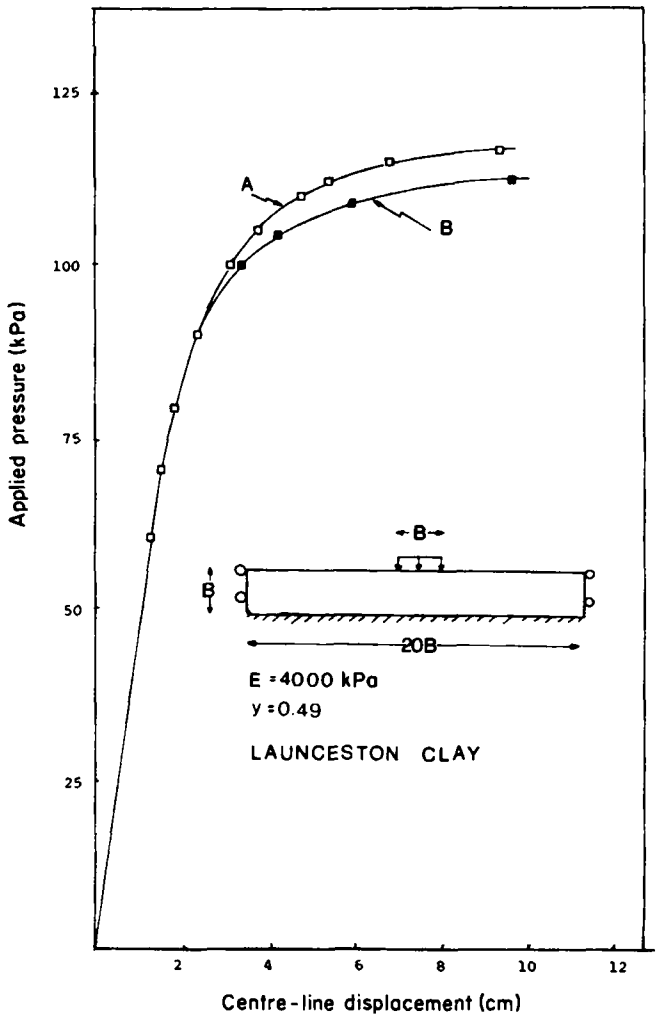

Figure 14. Load–deformation responses (infinitesimal strain). Curve A—Load–deformation response using the Launceston clay model without an initial stress field. Curve B—Load–deformation response using the Launceston clay model with an initial stress field of $\sigma_{\text{vertical}} = \gamma y$ and $\sigma_{\text{horizontal}} = 0{\cdot}8\ \gamma y$

ACKNOWLEDGEMENTS

The work reported herein was conducted while the authors were pursuing graduate studies at Monash University under the general supervision of Associate Professor I. B. Donald.

NOTATION

A = area
A_α = elemental area
c = cohesion
C_{ijkl}, $[C]$ = constitutive law
d_{ij} = rate of deformation tensor

$\bar{d}_{ij}$ = modified rate of deformation tensor
E = Young's modulus
F_i = body force vector
F_N = nodal component of body force
G = shear modulus
t = time
T_i = surface traction
T_N = nodal component of surface traction
u_k = displacement vector
V = volume
V_α = elemental volume
v_i = velocity vector
x_i = Eulerian coordinate
Y = uniaxial yield stress
ε_{ij} = natural strain tensor
κ = bulk modulus
ν = Poisson's ratio
σ_{ij} = stress tensor
$\dot{\sigma}_{ij}$ = stress rate tensor
$\overset{\nabla}{\sigma}_{ij}$ = Jaumann stress rate tensor
$\sigma_{o/b}$ = out of balance stresses
ϕ = independent dilational rate
Ω_{ij} = spin tensor
$\bar{\Omega}_{ij}$ = modified spin tensor

APPENDIX

Explicit forms of the finite element equations for the virtual power equation

The rate of deformation–nodal velocity equation is given by

$$\{d\} = [B]\{\dot{q}\} \tag{A1}$$

Under plane strain conditions

$$\{d\}^{\mathrm{T}} = \{d_x, d_y, d_{xy}\} \tag{A2}$$

and

$$[B] = \begin{bmatrix} \frac{\partial N_1}{\partial x} & 0 & \frac{\partial N_2}{\partial x} & 0 & \frac{\partial N_3}{\partial x} & 0 & \frac{\partial N_4}{\partial x} & 0 \\ 0 & \frac{\partial N_1}{\partial y} & 0 & \frac{\partial N_2}{\partial y} & 0 & \frac{\partial N_3}{\partial y} & 0 & \frac{\partial N_4}{\partial y} \\ \frac{\partial N_1}{\partial y} & \frac{\partial N_1}{\partial x} & \frac{\partial N_2}{\partial y} & \frac{\partial N_2}{\partial x} & \frac{\partial N_3}{\partial y} & \frac{\partial N_3}{\partial x} & \frac{\partial N_4}{\partial y} & \frac{\partial N_4}{\partial x} \end{bmatrix} \tag{A3}$$

The term $[T_w]\{\sigma\}$ is given by

$$\begin{bmatrix} 0 & 0 & \left(\frac{\partial v_y}{\partial x}-\frac{\partial v_x}{\partial y}\right) \\ 0 & 0 & -\left(\frac{\partial v_y}{\partial x}-\frac{\partial v_x}{\partial y}\right) \\ -\frac{1}{2}\left(\frac{\partial v_y}{\partial x}-\frac{\partial v_x}{\partial y}\right) & \frac{1}{2}\left(\frac{\partial v_y}{\partial x}-\frac{\partial v_x}{\partial y}\right) & 0 \end{bmatrix} \begin{Bmatrix} \sigma_x \\ \sigma_y \\ \tau_{xy} \end{Bmatrix} \tag{A4}$$

Explicit forms of the finite element equations for the mixed variational principle

The rate of deformation–nodal velocity equation is given by

$$\{\bar{d}\} = [\bar{B}]\{q\} \tag{A5}$$

Under plane strain conditions

$$\{\bar{d}\}^T = \{\bar{d}_x, \bar{d}_y, \bar{d}_{xy}\} \tag{A6}$$

and

$$[\bar{B}] = \begin{bmatrix} \frac{\partial N_1}{\partial x}+X_1 & Y_1 & \frac{\partial N_2}{\partial x}+X_2 & Y_2 & \frac{\partial N_3}{\partial x}+X_3 & Y_3 & \frac{\partial N_4}{\partial x}+X_4 & Y_4 \\ X_1 & \frac{\partial N_1}{\partial y}+Y_1 & X_2 & \frac{\partial N_2}{\partial y}+Y_2 & X_3 & \frac{\partial N_3}{\partial y}+Y_3 & X_4 & \frac{\partial N_4}{\partial y}+X_4 \\ \frac{\partial N_1}{\partial y} & \frac{\partial N_1}{\partial x} & \frac{\partial N_2}{\partial y} & \frac{\partial N_2}{\partial x} & \frac{\partial N_3}{\partial y} & \frac{\partial N_3}{\partial x} & \frac{\partial N_4}{\partial y} & \frac{\partial N_4}{\partial x} \end{bmatrix} \tag{A7}$$

where

$$X_i = \left[\frac{1}{3V_\alpha}\int_{V_\alpha}\frac{\partial N_i}{\partial x}\,dV\right] - \frac{1}{3}\left[\frac{\partial N_i}{\partial x}\right] \tag{A8}$$

$$Y_i = \left[\frac{1}{3V_\alpha}\int_{V_\alpha}\frac{\partial N_i}{\partial y}\,dV\right] - \frac{1}{3}\left[\frac{\partial N_i}{\partial y}\right] \tag{A9}$$

The term $[T_w]\{\sigma\}$ is written as

$$\begin{bmatrix} X & 0 & \left(\frac{\partial v_y}{\partial x}-\frac{\partial v_x}{\partial y}\right) \\ 0 & X & -\left(\frac{\partial v_y}{\partial x}-\frac{\partial v_x}{\partial y}\right) \\ -\frac{1}{2}\left(\frac{\partial v_y}{\partial x}-\frac{\partial v_x}{\partial y}\right) & \frac{1}{2}\left(\frac{\partial v_y}{\partial x}-\frac{\partial v_x}{\partial y}\right) & X \end{bmatrix} \begin{Bmatrix} \sigma_x \\ \sigma_y \\ \tau_{xy} \end{Bmatrix} \tag{A10}$$

where

$$X = \frac{2}{3}\left\{\frac{1}{V_\alpha}\int_{V_\alpha}\left(\frac{\partial v_x}{\partial x}+\frac{\partial v_y}{\partial y}\right)dV - \left(\frac{\partial v_x}{\partial x}+\frac{\partial v_y}{\partial y}\right)\right\} \tag{A11}$$

REFERENCES

1. O. C. Zienkiewicz, C. Humpheson and R. W. Lewis, 'Associated and non-associated visco-plasticity and plasticity in soil mechanics', *Geotechnique*, **25**, 671–689 (1975).
2. R. K. Rowe and E. H. Davis, 'Application of the finite element method to the prediction of collapse loads', *Res. Rep. No. R310*, Civil Engng Lab., Univ. of Sydney, Sydney (1971).
3. J. C. Nagtegaal, D. H. Parks and J. R. Price, 'On numerically accurate finite element solutions in the fully plastic range', *Computer Methods in Appl. Mech. Engng*, **14**, 153–177 (1974).
4. J. P. Carter, J. R. Booker and E. H. Davis, 'Finite deformation of an elasto-plastic soil', *Int. J. Numer and Anal. Methods Geomech.* **1**, 25–44 (1977).
5. C. T. Toh, 'Theoretical and experimental investigations into the behaviour of soft sensitive clays', *Ph.D. thesis*, Monash University, Melbourne, Australia (1978).
6. H. L. Davidson and W. F. Chen, 'Elastic–plastic large deformation response of clay to footing loads', Lehigh Univ., Fritz. Engng *Lab. Rep. No. 355*, 18, Bethelehem, Pennsylvania (1971).
7. H. V. Phan, C. S. Desai, S. Sture and J. V. Perumpral, 'Three-dimensional geometric and material nonlinear analysis of some problem in geomechanics', *Proc. 3rd Int. Conf. on Num. Method. Geomech.*, Aachen, West Germany (1979).
8. C. S. Desai and H. V. Phan, 'Three-dimensional finite element analysis including material and geometric nonlinearities', Invited paper, *2nd Int. Conf. on Comp. Meth. in Nonlinear Mech.*, Univ. of Texas, Austin (1979).
9. W. Prager, 'An elementary discussion of definition of stress rate', *A. Appl. Math.* **XVII** (4), 403–407 (1961).
10. C. Truesdell, *J. Nat. Mechs. Analys.* **2**, 593–616 (1953).
11. B. A. Cotter and R. S. Rivlin, 'Tensors associated with time-dependent stresses', *Q. Appl. Math.* **13**, 177–182 (1955).
12. A. E. Green, 'Hypoelasticity and plasticity', *Proc. Roy. Soc.* (*A*), **243**, 46–59 (1956).
13. G. Jaumann, *Grundlagen der Bewegungslehre*, Leipzig, 1905.
14. L. R. Hermann, 'Elasticity equations for incompressible and nearly incompressible materials by a variational theorem', *A.I.A.A. J.* **3**, 1896–1900 (1965).
15. G. C. Nayak and O. C. Zienkiewicz, 'Elasto-plastic stress analysis. A generalization for various constitutive relations including strain-softening', *Int. J. Num. Meth. Engng* **5**, 113–135 (1972).
16. R. M. Fernandez and J. T. Christian, 'Finite element analysis of large strains in soils', *Res. Report R71-37*, M.I.T. (1971).
17. P. G. Hodge and G. N. White, 'A quantitative comparison of flow and deformation theories of plasticity', *J. Appl. Mech.* **17**, 180.
18. R. Hill, *Mathematical Theory of Plasticity*, Oxford University Press, London, 1950.
19. W. F. Chen, *Limit Analysis and Soil Plasticity*. Elsevier, Amsterdam, 1975.